Emergent Fluctuation Hot Spots on the Fermi Surface of $CeIn_3$ in Strong Magnetic Fields

Takao Ebihara,[1] N. Harrison,[2] M. Jaime,[2] Shinya Uji,[3] and J. C. Lashley[2]
[1]*Department of Physics, Shizuoka University, Shizuoka 422-8529, Japan*
[2]*National High Magnetic Field Laboratory, Los Alamos National Laboratory, MS E536, Los Alamos, New Mexico 87545, USA*
[3]*National Institute of Material Science, Tsukuba, 305-0004, Japan*
(Received 17 June 2004; published 6 December 2004)

de Haas–van Alphen measurements on $CeIn_3$ in pulsed magnetic fields of up to 65 T reveal an increase in the quasiparticle effective mass with the field concentrated at "hot spots" on the Fermi surface as the Néel phase is suppressed. As well as revealing the existence of fluctuations deep within the antiferromagnetic phase, these data suggest that a possible new type of quantum critical point may exist in strong magnetic fields that involves only parts of the Fermi surface.

DOI: 10.1103/PhysRevLett.93.246401 PACS numbers: 71.45.Lr, 71.18.+y, 71.20.Ps

A quantum critical point (QCP) occurs when an ordered state of matter becomes unstable to quantum fluctuations at the absolute zero of temperature [1]. The possibility that quantum fluctuations resulting from a vanishing antiferromagnetic (AFM) order parameter could mediate novel forms of superconductivity remains the subject of considerable excitement [2,3]. $CeIn_3$ is a cubic AFM heavy fermion metal situated at the very heart of this debate [4,5], with a Néel temperature of $T_N \approx 10$ K and a staggered moment of $\approx 0.65\mu_B$ [6] close to the value $\approx 0.71\mu_B$ anticipated for localized Γ_7 doublets. T_N is suppressed under the application of hydrostatic pressure [4], with a concomitant increase in the Kondo temperature in accordance with Doniach's phase diagram [7–9]. Superconductivity then emerges at $T_c \approx 0.17$ K as T_N vanishes at a critical pressure of $p_c \approx 25$ kbar [4,5]. Evidence for quantum criticality at p_c includes an $n = \frac{3}{2}$ exponent in the electrical resistivity at low temperatures on fitting it to $\rho = \rho_0 + AT^n$ and a power law scaling of T_N of the form

$$T_N = T_{N,0} g^{\alpha_{p,B}}, \tag{1}$$

where $g_p = 1 - p/p_c$ and $\alpha_p \approx \frac{1}{3}$ [see Fig. 1(a)] [5,10–13]. In spite of these indications of quantum criticality, the experimental techniques applied to $CeIn_3$ thus far do not divulge the relation between the fluctuations and the Fermi surface (FS) topology: this would be necessary to determine whether the fluctuations occur uniformly over the FS or are concentrated in regions called "hot spots."

In this Letter, we show that T_N is also suppressed by a magnetic field $\mu_0 H \approx B = |\mathbf{B}|$, but in a quadratic fashion (to lowest order) such that $g_B = 1 - (B/B_c)^2$, $\alpha_B = 1.0 \pm 0.1$, and $B_c = 61 \pm 2$ T upon extrapolation. The same large B also furnishes well resolved Landau levels, enabling the extremal orbitally averaged quasiparticle effective mass m_o^* to be extracted directly from de Haas–van Alphen (dHvA) oscillations. Such experiments unambiguously reveal the fluctuations to be concentrated at hot spots on the FS of $CeIn_3$ [3,14], causing an increase in m_o^* on the approach to B_c only for certain orientations of $\mathbf{B}$. Such experiments enable the use of strong magnetic fields to probe quantum criticality in situations where the nonuniform distribution of the fluctuations over the FS and abundant spin-wave scattering [15,16] make conventional methods based on fitting values of A and the Sommerfeld coefficient γ (extracted from the heat capacity C) versus B inconclusive.

The $CeIn_3$ samples used in this study are grown in an alumina crucible inside an evacuated quartz tube using the self-flux method, yielding cubic single crystals of approximately 3 mm on a side. Annealing for 168 h at 950 °C reduces the residual resistivity to $\rho_0 \approx 0.6\ \mu\Omega$ cm (extrapolating ρ data below $T = 1.6$ K). The samples are then studied using a combination of etched single-crystal dHvA (cross section $<0.07\ \text{mm}^2$) and powdered-crystal magnetic susceptibility ($\chi = M/B$) techniques in magnetic fields of up to 65 T and tempera-

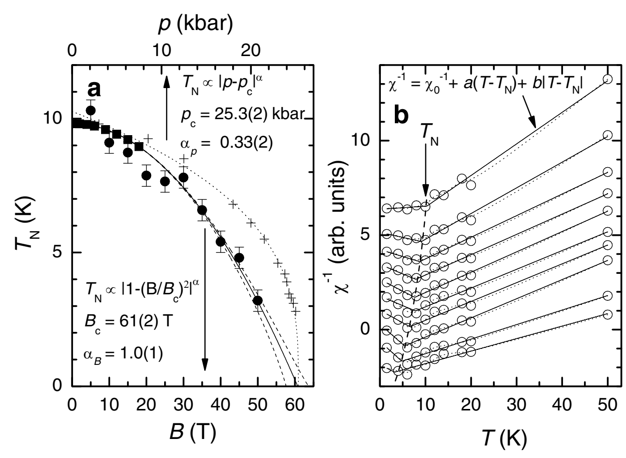

FIG. 1. Suppression of T_N in $CeIn_3$ by B and p. (a) T_N versus B extracted from C_{max} (squares) and the kink in χ^{-1} (circles), together with solid and dashed line fits, for $\alpha_B = 1$ and 1.0 ± 0.1, respectively. Also shown is T_N versus p data (crosses) from Mathur *et al.* [4] with a dotted line fit. (b) χ^{-1} as a function of T at different magnetic fields, together with solid line fits.

tures T down to ≈ 0.4 K. Proportionality of the dHvA signal to $\partial B/\partial t$ at each T and B confirm the absence of significant eddy current heating. Low field measurements of the dHvA effect and of C are made in superconducting magnets.

Figure 1(a) compares the suppression of T_{N} by p observed by Mathur *et al.* [4] with that by B observed in the present work. In the former case, the fitting of Eq. (1) (dotted line) to the data points ("+" symbols) extracted from the kink in the T dependence of ρ at T_{N} yields $\alpha_p = 0.33 \pm 0.02 \approx \frac{1}{3}$ and $p_{\mathrm{c}} = 25.3 \pm 0.2$ kbar. In the latter case, data points (squares) extracted from the maximum $C_{\max}$ of the anomaly in C yield a quadratic dependence of T_{N} on B (solid line) to the highest magnetic fields of 18 T in Fig. 1(a) to which C is measured. The χ^{-1} data shown in Fig. 1(b), obtained from many magnet pulses to 55 T at different temperatures, enable the dependence of T_{N} on B to be followed to higher magnetic fields. T_{N} manifests itself as a kink in χ^{-1} (circles), which can be approximately reproduced by an "elbow" function of the form $\chi^{-1} = \chi_0^{-1} + a(T - T_{\mathrm{N}}) + b|T - T_{\mathrm{N}}|$ in Fig. 1(b). T_{N} data points extracted from the kink data (circles) continue to follow the quadratic extrapolation (solid line for $\alpha_B = 1$) of the $C_{\max}$ versus B data points in Fig. 1(a), albeit with increased scatter. Dashed lines correspond to the fits obtained on adjusting α_B by 10%, while maintaining $\alpha_B/B_{\mathrm{c}}^2$ constant so as not to significantly affect the gradient for $B < 18$ T. The C and χ^{-1} data together therefore suggest that $\alpha_B = 1.0 \pm 0.1$, introducing a great uncertainty in the slope $0 < -\partial T_{\mathrm{N}}/\partial B < \infty$ of the phase boundary at $B_{\mathrm{c}} = 61 \pm 2$ T as $T_{\mathrm{N}} \rightarrow 0$. Since $\alpha_B \gg \alpha_p$, T_{N} is much more likely to remain second order as $g_B \rightarrow 0$ than for $g_p \rightarrow 0$, making it a strong candidate for quantum criticality. A vanishing $\partial T_{\mathrm{N}}/\partial B$ as $T_{\mathrm{N}} \rightarrow 0$, may possibly explain the absence of a discernible jump in the magnetization M at B_{c} in Fig. 2(a) above the level of the experimental noise.

Evidence for an ensuing QCP often manifests itself as a divergence in γ on the approach to B_{c} [17] or p_{c} [3], and in A on the condition that $\gamma^2/A = \text{const}$ [18]. Estimates of γ and A become somewhat subjective in AFM metals, however, owing to the absence of a fully comprehensive model for spin-wave scattering [10,12,19,20]. Furthermore, neither γ nor A can be used to locate hot spots in k space.

By enabling m_{o}^* to be measured directly for different extremal orbits around the FS, dHvA experiments provide an ideal means with which to verify the existence of hot spots. The published $\mathrm{CeIn_3}$ dHvA data are consistent with the existence of such hot spots on the FS situated at $\mathbf{k}_{\mathrm{hot}} = [\pm\frac{1}{\sqrt{3}}, \pm\frac{1}{\sqrt{3}}, \pm\frac{1}{\sqrt{3}}]k_{\mathrm{F}}$ (depicted in Fig. 3), where $k_{\mathrm{F}} \approx 3.0 \times 10^9\ \mathrm{m}^{-1}$ is the Fermi wave vector of the largest approximately spherical section of FS observed within the AFM phase [14]. When the sample is oriented such that the extremal orbit of the quasiparticles moving in the plane orthogonal to $\mathbf{B}$ avoids these hot spots (e.g., $\mathbf{B} \parallel \langle 100\rangle$), m_{o}^* is found to be $\approx 2m_{\mathrm{e}}$ (i.e., only twice the free electron mass [14]) and approximately independent of B. When the orientation of the sample is changed so as to cause the quasiparticles to pass directly through the hot spots (e.g., $\mathbf{B} \parallel \langle 110\rangle$), however, m_{o}^* abruptly increases to $\approx 12m_{\mathrm{e}}$. Because $m_{\mathrm{o}}^* = \frac{1}{2\pi}\oint(m^*(\mathbf{k})/k_{\mathrm{F}})dk \approx \frac{4}{12}m^*(\mathbf{k}_{\mathrm{hot}}) + (1 - \frac{4}{12})m^*(\mathbf{k}_{\mathrm{cold}})$ is an orbital average that includes regions between the hot spots where $m^*(\mathbf{k}_{\mathrm{cold}}) \approx 2m_{\mathrm{e}}$, the local effective mass $m^*(\mathbf{k}_{\mathrm{hot}})$ at $\mathbf{k}_{\mathrm{hot}}$ must have a value of $\sim 32m_{\mathrm{e}}$ to account for $m_{\mathrm{o}}^* \approx 12m_{\mathrm{e}}$ at this orientation (noting that the width of each hot spot occupies approximately $\frac{1}{12}$ of the circumference of the FS [14]).

Thermal damping of the dHvA oscillations by a factor $R_T(T/B) = X/\sinh X$, where $X = 2\pi^2 m_{\mathrm{o}}^* k_{\mathrm{B}} T/\hbar e B$ [21], restricts the observation of dHvA oscillations to orbits with $m_{\mathrm{o}}^* \lesssim 12m_{\mathrm{e}}$ for $T \gtrsim 400$ mK in the present study. dHvA oscillations can therefore be observed only along the symmetry directions $\mathbf{B} \parallel \langle 100\rangle$ and $\mathbf{B} \parallel \langle 111\rangle$ in Fig. 2(b). Fits (dotted lines) of $R_T(T/B)$ to the Fourier amplitudes (open symbols) of the dHvA signal over different ~ 10 T wide intervals in magnetic field in Fig. 4(a) show that the dependence of $R_T(T/B)$ on T/B is comparatively weak and varies little with B for $\mathbf{B} \parallel \langle 100\rangle$, i.e., when the orbit avoids the hot spots. This is consistent with $m^*(\mathbf{k}_{\mathrm{cold}})$ being weakly dependent on field over the majority of the spherical FS [see Fig. 4(b)]. In contrast,

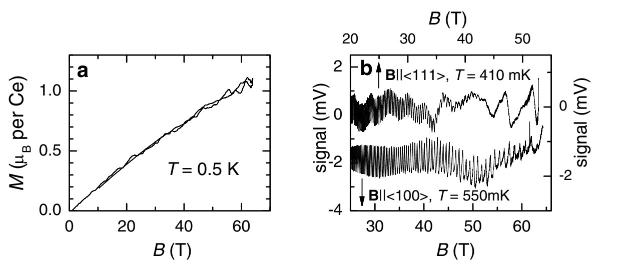

FIG. 2. (a) An example of the magnetization M of $\mathrm{CeIn_3}$ powder. (b) Examples of raw dHvA data for $\mathbf{B} \parallel \langle 100\rangle$ and $\mathbf{B} \parallel \langle 111\rangle$: for the latter, the signal already vanishes at ~ 44 T due to the increase in m_{o}^*, before the peak of the magnetic field pulse where $\partial B/\partial t = 0$ is reached.

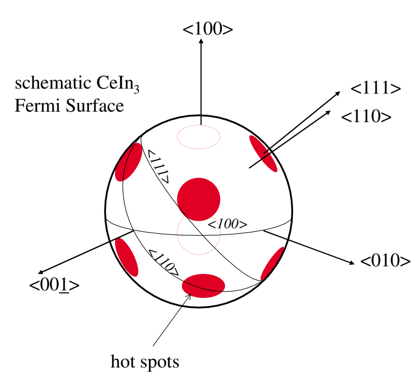

FIG. 3 (color online). A schematic of the near spherical d-FS sheet of $\mathrm{CeIn_3}$, illustrating the passage of the extremal quasiparticle orbits with respect to the hot spots for different orientations of $\mathbf{B}$.

similar fits (dashed lines and filled symbols) for $\mathbf{B} \parallel \langle 111 \rangle$ reveal a clear trend of increasing steepness as B is increased, caused by a significant increase in m_o^* [see Fig. 4(b)]. A moderately enhanced m_o^* is observed for $\mathbf{B} \parallel \langle 111 \rangle$ because the orbit just about intersects the hot spots at that orientation. An enhanced and increasing m_o^* observed for $\mathbf{B} \parallel \langle 111 \rangle$ but not for $\mathbf{B} \parallel \langle 100 \rangle$, suggests that only $m^*(\mathbf{k}_{\rm hot})$ increases with field. An increase in m_o^* with field for any orbit that passes through or near a hot spot is therefore the direct consequence of an increase in $m^*(\mathbf{k}_{\rm hot})$. Hence, while the largest orbitally averaged mass of $m_o^* = (6.77 \pm 0.35)m_e$ for $\mathbf{B} \parallel \langle 111 \rangle$ is rather modest compared to other heavy fermion materials, the $[(m_{o,111}^* - m_{o,100}^*)_{B=42\,{\rm T}}/(m_{o,111}^* - m_{o,100}^*)_{B=14\,{\rm T}} = 9 \pm 2]$-fold increase in the difference in mass between $\mathbf{B} \parallel \langle 111 \rangle$ and $\mathbf{B} \parallel \langle 100 \rangle$ (which can be attributed to fluctuations at the hot spots) suggests a (9 ± 2)-fold increase in the hot spot mass $m^*(\mathbf{k}_{\rm hot})$ to $\sim(270 \pm 50)m_e$at 42 T.

The electronic states for any given band in a Fermi liquid are filled up to the Fermi energy $\varepsilon_{\rm F} = \hbar eF/m_o$. Parabolicity of the electronic bands, in the case of noninteracting electrons, exacts a direct proportionality between the orbitally averaged band mass m_o and the extremal FS cross section $A_k = (2\pi e/\hbar)F$. The observation of large angular variations in m_o^* in $CeIn_3$ without any significant variation in A_k [14] cannot be explained by a noninteracting electron picture, implying that the variations in $m^*(\mathbf{k})$ are the direct consequence of many-body interactions. Such interactions, caused by coherent scattering, are generally expected to enhance m_o^* observed in dHvA experiments [22–24], while preserving the functional form of $R_T(T/B)$. This enables us to define an effective Fermi energy scale $\varepsilon_{\rm F}^* = \hbar eF/m_o^*$ for each

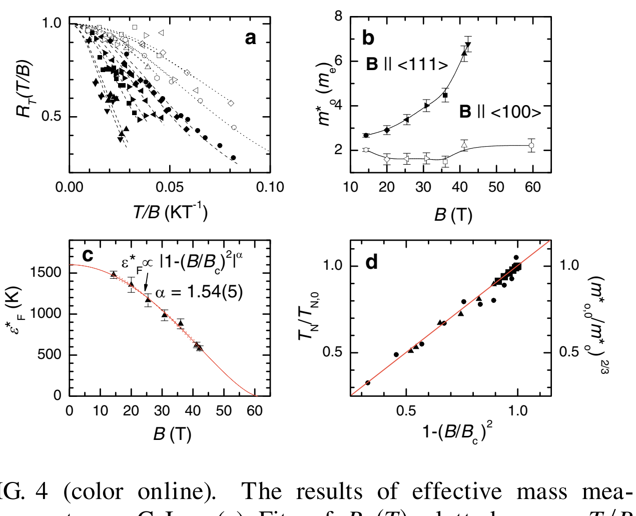

FIG. 4 (color online). The results of effective mass measurements on $CeIn_3$. (a) Fits of $R_T(T)$ plotted versus T/B for $\mathbf{B} \parallel \langle 100 \rangle$ (open symbols) and $\mathbf{B} \parallel \langle 111 \rangle$ (solid symbols). (b) m_o^* versus B for $\mathbf{B} \parallel \langle 100 \rangle$ and $\mathbf{B} \parallel \langle 111 \rangle$, where different symbols refer to different fits in (a). (c) The effective Fermi energy scale $\varepsilon_{\rm F}^*$ estimated using Eq. (2) for $\mathbf{B} \parallel \langle 111 \rangle$, with a fit as described in the text. (d) A plot showing generic scaling between $T_{\rm N}$, m_o^*, and $g = 1 - (B/B_c)^2$ with squares, circles, and triangles representing $C_{\rm max}$, χ^{-1}, and m_o^* data, respectively.

extremal orbit that depends on the extent to which m_o^* is enhanced by fluctuations. The reduction of $\varepsilon_{\rm F}^*$ as $B \rightarrow B_c$ for $\mathbf{B} \parallel \langle 111 \rangle$ in Fig. 4(c) is consistent with the possible existence of a QCP at B_c upon extrapolation. The solid line represents a fit to

$$\varepsilon_{\rm F}^* \equiv \frac{\hbar eF}{m_o^*} = \varepsilon_{{\rm F},0}^* g^{\alpha'}, \qquad (2)$$

where $g_B = 1 - (B/B_c)^2$ as for $T_{\rm N}$ versus B, but where $\alpha' = 1.54 \pm 0.05$. The reliability of the estimate of α' from this two parameter fit can be assessed by performing additional single parameter fits with α' fixed to 1.44 and 1.64, giving dotted lines in Fig. 4(c) that match the error bars of the highest magnetic field data points. One simple expectation of such a power law fit to g_B is that $\varepsilon_{\rm F}^*$ should collapse to zero as m_o^* diverges at B_c. The present limitations of the dHvA experiments imply that verification of quasiparticle divergencies would require T-dependent ρ and C measurements to be made at B_c. The fit to Eq. (2) nevertheless suggests a scaling relation of the form

$$\frac{\varepsilon_{\rm F}^*}{\varepsilon_{{\rm F},0}^*} = \frac{m_{o,0}^*}{m_o^*} = \left(\frac{T_{\rm N}}{T_{{\rm N},0}}\right)^{\alpha'/\alpha_B} \qquad (3)$$

in Fig. 4(d) (where $\alpha'/\alpha_B \sim \frac{3}{2}$), implicating the AFM order parameter as the source of the fluctuations that contribute to m_o^* at low temperatures.

While the dHvA oscillations vanish before B_c is reached for $\mathbf{B} \parallel \langle 111 \rangle$, the continued observation of a dHvA signal at and possibly above B_c for $\mathbf{B} \parallel \langle 100 \rangle$ raises interesting questions concerning the nature of the FS transformation that occurs at the putative field-tuned QCP. The absence of any apparent attenuation of the dHvA signal in the vicinity of B_c at this orientation in Fig. 2(b) suggests that light sections of FS survive the putative QCP intact. Both m_o^* in Fig. 4(b) and F evaluated from Fourier transforms over the field interval $55 < B < 65$ T (which includes B_c within experimental error), remain unchanged to within $\sim$5% of their low field values (a precision that is limited only by the small finite number of oscillations). Were the $4f$ electrons to become itinerant when $B > B_c$, as is thought to occur at $B = 0$ and $p > p_c$ [3], the FS volume would have to change at B_c so as to accommodate one additional electron per formula unit within the conduction band of $CeIn_3$ [3]. In $CeRhIn_5$, where quantum criticality is also thought to be tuned by p (with $B < 20$ T), the entire FS is reported to change at p_c [25]. Until a similar complete FS change is observed in $CeIn_3$ at high magnetic fields, alternative scenarios should be considered. One such alternative scenario is that $4f$ electrons in $CeIn_3$ continue to remain effectively localized at $B > B_c$ owing to the polarization of the $4f$ bands in strong magnetic fields. The large value of the magnetization per Ce ion in Fig. 2(a), which is tending towards saturation, might be consistent with such a scenario.

In order to understand the origin of fluctuations only at $\mathbf{k}_{\rm hot}$, it is instructive to compare the FS of $CeIn_3$ [14] with that of $LaIn_3$ [26]. Prior dHvA studies had concluded that the largest sheet of FS in $CeIn_3$ corresponds to a similarly sized sheet situated at the Γ point, labeled d in $LaIn_3$ [14], as a consequence of the $4f$ electrons being localized within the AFM phase [6]. One essential difference between the FSs, however, is that the d sheet of $LaIn_3$ possesses necks at $\mathbf{k}_{\rm neck} \approx [\pm\frac{1}{\sqrt{3}}, \pm\frac{1}{\sqrt{3}}, \pm\frac{1}{\sqrt{3}}]k_{\rm F}$ that protrude from the otherwise spherical FS to connect to other portions of FS [26]. These portions of FS would lie outside the AFM Brillouin zone of $CeIn_3$ (which is $\frac{1}{8}$ the size of that of nonmagnetic $LaIn_3$) [6], implying that the necks in $CeIn_3$ must be truncated as a consequence of Bragg reflection of the quasiparticles off the AFM ordered $4f$ moments.

The process by which the FS is modified by Bragg reflection here is therefore qualitatively similar to that accompanying spin-density wave (SDW) formation as described by Hertz and Millis [27]. One essential difference here, however, is that the fluctuations and Bragg reflections are associated with an AFM phase formed from $4f$ electrons that are localized and coupled via RKKY interactions rather than a SDW. No exchange of charge degrees of freedom takes place between the conduction electrons and $4f$ electrons in such a scenario. Bragg reflection, nevertheless, still causes gaps to open on the conduction electron FS, leading to a weak conduction electron spin modulation that may compete with that of the ordered $4f$ moments [6]. Necks like those in $LaIn_3$ must eventually reappear in $CeIn_3$ as soon as $T_{\rm N} \rightarrow 0$, which would cause the dHvA signal to vanish for orientations of $\mathbf{B}$ where the quasiparticle orbit is interrupted by the necks (i.e., along symmetry directions $\mathbf{B} \parallel \langle 111 \rangle$ and $\mathbf{B} \parallel \langle 110 \rangle$), as is the case in $LaIn_3$. Note that the location of the necks on the FS of $LaIn_3$ coincides with the location of the hot spots in $CeIn_3$, implying that the fluctuations at the hot spots must be associated with the change in FS that takes place only at the necks as a consequence of the AFM order parameter.

In summary, we show that the suppression of $T_{\rm N}$ by B in $CeIn_3$ is accompanied by an increase in fluctuations associated with the AFM order parameter concentrated at hot spots on the FS. These give rise to an increase in $m^*_{\rm o}$ for orbits that pass through or near the hot spots, which is consistent with the existence of a possible QCP involving these hot spots at $\approx$61 T. While it is expected that a heavy composite Fermi liquid with itinerant $4f$ electrons exists at $p > p_{\rm c}$ and $B = 0$ [3–5], the limited data set presented in this Letter thus far appears to be consistent with a different scenario in strong magnetic fields in which light sections of FS survive the putative QCP intact. One possibility is that the $4f$ electrons remain localized at $B > B_{\rm c}$ and $p = 0$. Further experiments are necessary to address the evolution of the putative QCP versus p and B as well as the itinerant-versus-localized state of the $4f$ electrons and FS topology in the region of phase space immediately outside the AFM phase.

This work is supported by the National Science Foundation, the Department of Energy, and Florida State. The work at Japan National Institute for Materials Science is supported by Japanese Ministry of Education. One of the authors (T. E.) is supported, in part, by Corning Japan and CASIO Science Promotion Foundation.

[1] S. Sachdev, *Quantum Phase Transitions* (Cambridge University Press, Cambridge, 1999).
[2] R. B. Laughlin *et al.*, Adv. Phys. **50**, 361 (2001).
[3] P. Coleman *et al.*, J. Phys. Condens. Matter **13**, R723 (2001).
[4] N. D. Mathur *et al.*, Nature (London) **394**, 39 (1998).
[5] F. M. Grosche *et al.*, J. Phys. Condens. Matter **13**, 2845 (2001).
[6] J. M. Lawrence, and S. M. Shapiro, Phys. Rev. B **22**, 4379 (1980).
[7] C. Thessieu *et al.*, Physica (Amsterdam) **281-282B**, 9 (2000).
[8] G. Knebel *et al.*, Phys. Rev. B **65**, 024425 (2001).
[9] S. Doniach, Physica (Amsterdam) **91B**, 231 (1977).
[10] K. Ueda, J. Phys. Soc. Jpn. **43**, 1497 (1977).
[11] A. Rosch, Phys. Rev. Lett. **82**, 4280 (1999).
[12] S. N. de Medeiros *et al.*, Physica (Amsterdam) **281-282B**, 340 (2000); M. A. Continentino *et al.*, Phys. Rev. B **64**, 012404 (2001).
[13] M. J. Steiner *et al.*, J. Magn. Magn. Mater. **226-230**, 333 (2001).
[14] T. Ebihara *et al.*, J. Phys. Soc. Jpn. **61**, 1473 (1992); T. Ebihara *et al.*, Physica (Amsterdam) **186-188B**, 123 (1993).
[15] I. R. Walker *et al.*, Physica (Amsterdam) **282-287C**, 303 (1997).
[16] G. Knebel *et al.*, High Press. Res. **22**, 167 (2002).
[17] P. Gegenwart *et al.*, Phys. Rev. Lett. **89**, 056402 (2002); J. Custers *et al.*, Nature (London) **424**, 524 (2003).
[18] K. Kadowaki and S. Woods, Solid State Commun. **58**, 507 (1986).
[19] C. Akiba and T. Mitsui, Solid State Commun. **13**, 1737 (1973).
[20] I. Balberg and A. Maman, Physica (Amsterdam) **96B**, 54 (1979).
[21] D. Shoenberg, *Magnetic Oscillations in Metals* (Cambridge University Press, Cambridge, 1984).
[22] G. G. Lonzarich, J. Magn. Magn. Mater. **76-77**, 1 (1988).
[23] S. Engelsberg and G. Simpson, Phys. Rev. B **2**, 1657 (1970).
[24] A. Wasserman and M. Springford, Adv. Phys. **45**, 471 (1996).
[25] H. Shishido *et al.*, in Proceedings of the International Conference on Strongly Correlated Electrons Systems, Karlsruhe, 2004 (to be published).
[26] I. Umehara, N. Nagai, and Y. Onuki, J. Phys. Soc. Jpn. **60**, 591 (1991).
[27] J. A. Hertz, Phys. Rev. B **14**, 1165 (1976); A. J. Millis, Phys. Rev. B **48**, 7183 (1993); T. Moriya *et al.*, J. Phys. Soc. Jpn. **64**, 960 (1995).